THE JOURNAL OF PHYSICAL CHEMISTRY B

Article

pubs.acs.org/JPCB

Asymmetric Squaraine Dyes: Spectroscopic and Theoretical Investigation

K. M. Shafeekh,[†] Suresh Das,[†] Cristina Sissa,[‡] and Anna Painelli[‡]

[†]Photosciences and Photonics Section, Chemical Sciences and Technology Division, National Institute for Interdisciplinary Science and Technology (CSIR-NIIST), Trivandrum 695019, India

[‡]Dipartimento di Chimica, Parma University & INSTM UdR-Parma, I-43100 Parma, Italy

Supporting Information

ABSTRACT: A joint experimental and theoretical study is presented of two asymmetric squaraine dyes and their parent symmetric dyes. The definition of reliable essential-state models for asymmetric squaraines sheds light on the intriguing spectroscopic behavior of this class of molecules, showing inverted and normal solvatochromism in absorption and emission, respectively. This behavior is related to charge redistribution in the excited state, with important implications for optimal design of asymmetric dyes for solar cell applications.

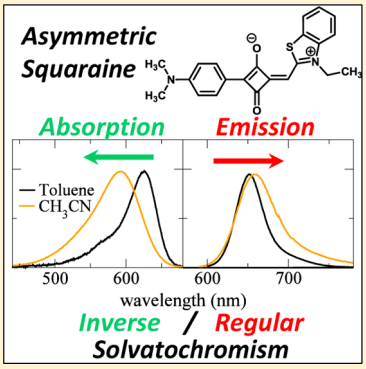

INTRODUCTION

π-Conjugated chromophores are attracting considerable attention as promising building blocks for molecular functional materials with applications in organic electronics, photovoltaics, and photonics due to the presence of delocalized electrons that ensure nonlinear response to external stimuli and smart behavior.[1−6] Squaraine-based dyes are particularly interesting π-conjugated chromophores due to their intense absorption and fluorescence in the red region of the optical spectrum[7−13] and their large nonlinear optical responses,[14−24] including two-photon absorption and third-harmonic generation. Recently, squaraine dyes have been extensively investigated as light-absorbers in organic photovoltaic (OPV) applications[25−32] and dye-sensitized solar cells (DSSC).[33−40] The central core of squaraines is a four-membered ring derived from the squaric acid that behaves as a strong electron-acceptor group (**A**). This central unit is linked to two electron-donating groups in a $\mathbf{D_L}-\mathbf{A}-\mathbf{D_R}$ structure that is symmetric when the two donor groups are the same ($\mathbf{D_L} = \mathbf{D_R}$) or asymmetric when $\mathbf{D_L} \neq \mathbf{D_R}$. Asymmetric squaraine dyes are investigated as NIR probes[41−45] and for applications in solar cells.[30−40] Two main reasons make asymmetric squaraines interesting for solar cells: (a) the presence of different lateral groups can facilitate a directional chemical binding to the relevant material (like the titania substrate in DSSC) and (b) the very intense but sharp absorption band typical of symmetric squaraine dyes becomes broader in asymmetric squaraines, with a better overlap with the solar spectrum and hence improved cell efficiency.

Several studies have addressed the electronic structure of symmetric and asymmetric squaraine dyes,[46−52] and it is now well recognized that TD-DFT, which in general works very well for π-conjugated dyes, does not offer a reliable description of the excitation spectrum of most dyes belonging to this notable class of molecules.[50] As thoroughly discussed in refs 47−49, this is most probably related to the biradicalic character of low-lying excitations in squaraines. On a more general vein, high-quality first-principle calculations for description of electronic excitations and their evolution with solvent polarity are still in their infancy and computationally highly demanding for large chromophores.[53] Phenomenological essential-state models offer an alternative, simple, and effective interpretative tool for low-energy optical spectra of organic chromophores. Essential-state models adopt a minimal basis set to describe the electronic structure of the dye and explicitly introduce coupling of electronic degrees of freedom to molecular vibrations and an effective solvation coordinate. Recent studies, based on very high quality quantum chemical calculation, convincingly demonstrate the applicability of essential-state models to specific families of dyes, opening the way to the ab initio definition of relevant model parameters.[54] While interesting, these approaches are extremely expensive and we prefer to stick on a much simpler phenomenological approach, extracting model parameters from careful analysis of optical spectra. Along these lines, we were able to rationalize and reproduce linear and nonlinear optical properties of several families of organic dyes.[51,52,55−60] Specifically, symmetric squaraine dyes are described as representative of the large family of quadrupolar dyes, and more precisely, they are classified as class II

Received: January 31, 2013
Revised: May 20, 2013
Published: June 18, 2013

   dx.doi.org/10.1021/jp401099g | J. Phys. Chem. B 2013, 117, 8536−8546

quadrupolar dyes,[51] not undergoing symmetry breaking in either the ground or the excited state. Within this framework we were able to rationalize the marginal solvatochromism shown by symmetric squaraines, their narrow spectral features, as well as their very intense (resonantly amplified) two-photon absorption (2PA) toward a state whose energy is roughly twice as large as the energy of the one-photon absorption (1PA).[51] Stimulated by the success of essential-state models to describe symmetric squaraine dyes, we present here a detailed spectroscopic study and theoretical analysis of asymmetric squaraine dyes. In particular, two asymmetric squaraines, D_1−A−D_2 and D_1−A−D_3 (Chart 1) have been synthesized and

Chart 1. Molecular Structures Subject of Analysis

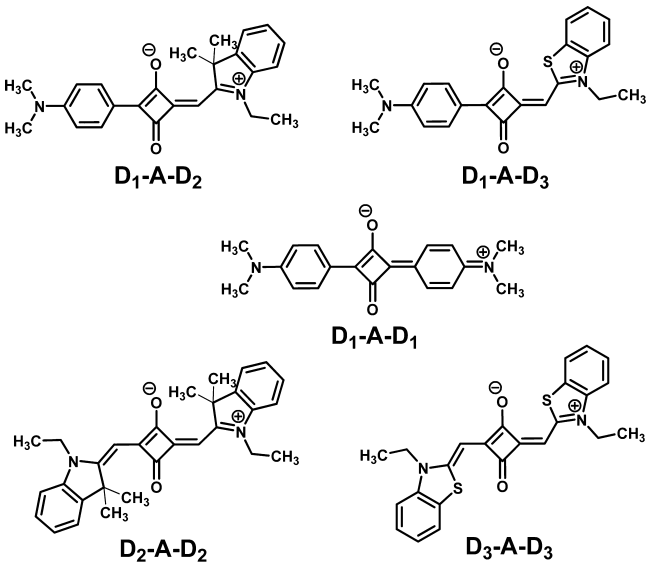

spectroscopically characterized. These asymmetric molecules have different electron-donor groups and different π-conjugated bridges on each arm, leading to strongly asymmetric structures. For the sake of comparison, the corresponding symmetric structures D_1−A−D_1, D_2−A−D_2, and D_3−A−D_3 have also been investigated: as expected on physical grounds, asymmetric dyes show a qualitatively different optical behavior with respect to their symmetric analogues. Analysis of optical spectra of symmetric dyes allows for robust parametrization of the relevant models, offering a safe basis to analyze optical spectra of asymmetric dyes.

EXPERIMENTAL SECTION

Squaric acid, 2-methyl-1,3-benzothiazole, and 2,3,3-trimethylindolenine were purchased from Sigma Aldrich. All other chemicals and solvents used were of highest available purity and have been obtained from Indian companies. ^{1}H and ^{13}C NMR spectra were recorded on a Bruker 500/300 MHz NMR spectrometer. FAB-MS were measured on a JEOL JMS 600H mass spectrophotometer. Absorption measurements were carried out in a Shimadzu UV-3101 PC UV−vis−NIR Scanning Spectrophotometer, and steady state flourescence measurements were done in a Spex Fluorolog 112X spectroflourimeter. Compound **1** was synthesized using a reported procedure as shown in Scheme 1.[63]

Synthesis of *N*-Ethyl-2,3,3-trimethyl Indolenine (D_2), Scheme 1. To 1.0 g (6.28 mmol) of 2,3,3-trimethylindolenine in 3 mL of acetonitrile in a pressure tube, 1.0 mL (12.18 mmol)

Scheme 1. Synthesis of 1, D_2 and D_3

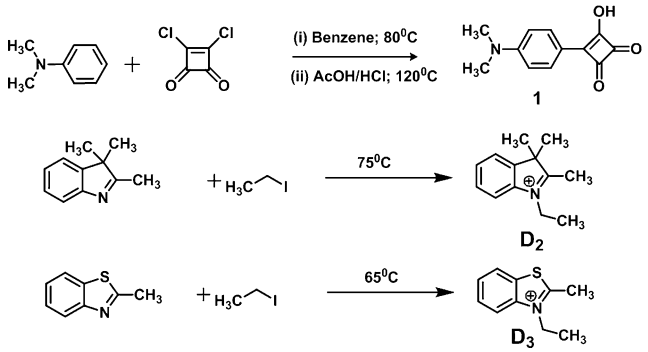

of ethyl iodide was added and the mixture was heated for 75 °C for 12 h. The mixture was concentrated in vacuo, and the product was purified by repeated precipitation from methanol using diethyl ether.

^{1}H NMR (300 MHz, CD_3OD): 7.89−7.86 (d, 1H, J = 8.5 Hz, aromatic), 7.79−7.76 (d, 1H, 8.5 Hz, aromatic), 7.67−7.63 (m,2H, aromatic), 4.53−4.60 (q, 2H, N−CH_2), 3.29 (s, 3H), 1.60 (s, 6H), 1.54−1.59 (t, 3H) ppm. ^{13}C NMR (75 MHz): 142.16, 129.83, 129.14, 123.32, 115.03, 54.56, 43.43, 21.35, 11.89 ppm. FAB-MS: calcd, 188.14; found, 188.27.

Synthesis of *N*-Ethyl-2-methyl-1,3-benzothiazole (D_3), Scheme 1. To 2.0 g (13.4 mmol) of 2-methyl-1,3-benzothiazole in a pressure tube, 2.2 mL (26.8 mmol) of ethyl iodide was added. The mixture was heated for 65 °C for 8 h. Solid obtained was washed with diethyl ether and then dissolved and precipitated from methanol using diethyl ether.

^{1}H NMR(500 MHz, CD_3OD): 8.33−8.31 (d, 1H, J = 8.0 Hz, aromatic), 8.29−8.27 (d, 1H, 8.5 Hz, aromatic), 7.93−7.90 (q, J = 8.5 Hz, 1H, aromatic), 7.83−7.80 (q, J = 8.0 Hz, 1H, aromatic), 4.83−4.79 (q, 2H, −N−CH_2), 3.30 (s, 3H), 1.60 (s, 3H) ppm. ^{13}C NMR (125 MHz, CD_3OD): 177.94, 142.33, 131.07, 130.86, 129.79, 125.4, 117.78, 48.68, 46.43, 16.98 ppm. FAB-MS: calcd,178.27; found, 178.37

Synthesis D_3−A−D_3 (Scheme 2). D_3−A−D_3 was synthesized by refluxing a mixture of *N*-ethyl-2-methyl-1,3-benzothiazole (0.20 g; 1.12 mmol) and squaric acid (0.06 g; 0.56 mmol) in a mixture of 2:1 butanol:benzene in the presence of 1 mL of quinoline fitted with a Dean Starck condenser for azeotropic removal of water for about 6 h. After cooling, the reaction mixture was concentrated to 2 mL and precipitated by adding an excess of hexane. It was then filtered, and the product was purified by column chromatography using silica gel (100−200 mesh) with 1% methanol−chloroform to yield 75 mg (15%) of the pure product.

^{1}H NMR (300 MHz, CD_3OD): 7.54−7.57 (d, 1H, J = 7.5 Hz, aromatic), 7.36−7.39 (d, 1H, 7.8 Hz, aromatic), 7.14−7.24 (m, 2H, aromatic), 5.91 (s, 1H, olefinic), 4.16−4.19 (q, 2H, $^+$N−CH_2), 1.44−1.46 (t, 3H) ppm. ^{13}C NMR (125 MHz): 173.43, 159.69, 140.72, 128.66, 127.31, 124.21, 122.37, 111.33, 100.13, 41.22, 29.76, 12.32 ppm. FAB-MS: calcd, 432.10; found, 432.63.

Synthesis of D_1−A−D_2 (Scheme 2). D_1−A−D_2 was synthesized by refluxing a mixture of *N*,*N*-dimethylaniline semisquaraine (0.20 g; 0.92 mmol) and *N*-ethyl-2,3,3-trimethyl indolenine (0.17g; 0.92 mmol) in a mixture of 2:1 butanol:benzene fitted with a Dean Starck trap for azeotropic removal of water for about 6 h. After cooling, the reaction mixture was concentrated to 2 mL and precipitated by adding

dx.doi.org/10.1021/jp401099g | J. Phys. Chem. B 2013, 117, 8536−8546

Scheme 2. Synthesis of D_3–A–D_3, D_1–A–D_3 and D_1–A–D_2

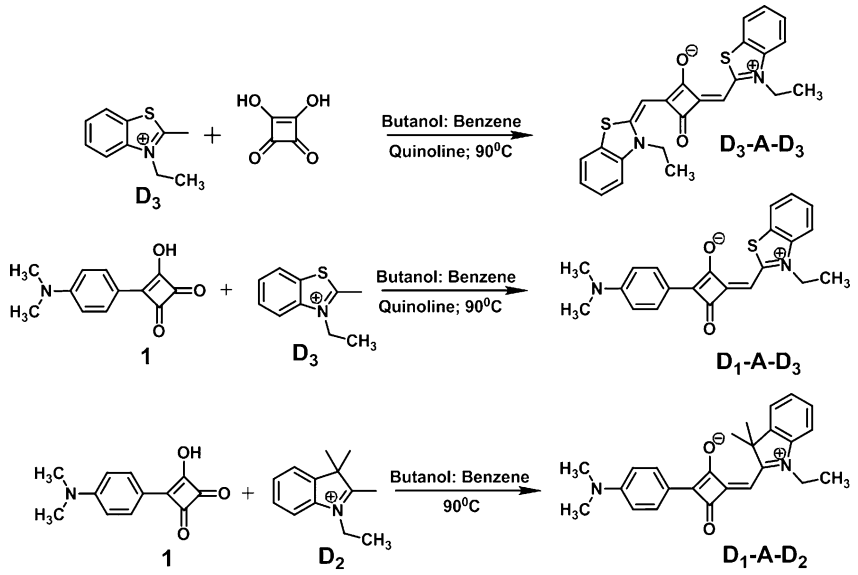

excess hexane. It was then filtered, and the product was purified by column chromatography using silica gel (100–200 mesh) with 1% methanol–chloroform to yield 100 mg (28%) of the pure product.

^{1}H NMR (300 MHz, $CDCl_3$): 8.26–8.29 (d, 2H, J = 8 Hz), 7. 35–7. 44 (m, 2H), 7.27–7.29 (d, 1H, J = 7.5 Hz) 7.13–7.15 (d, 1H, J = 7.8 Hz), 6.70–6.73 (d, 2H, 8.0 Hz, aromatic), 6.17 (s, 1H, olefinic), 4.18–4.25 (q, 2H, +N–CH_2), 3.10 (s, 6H, $N(CH_3)_2$),1.82 (s, 6H,$C(CH_3)_2$), 1.42–1.47 (t, 3H) ppm. ^{13}C NMR (125 MHz): 189.83, 180.96, 175.30, 174.89, 152.80, 143.03, 141.15, 130.87, 128.18, 125.70, 122.65, 119.79, 111.87. 110.61, 88.79, 50.71, 40.16, 26.46, 12.49 ppm. FAB-MS (M + 1): calcd, 386.20; found, 387.48

Synthesis of D_1–A–D_3 (Scheme 2). D_1–A–D_3 was synthesized by refluxing a mixture of *N,N*-dimethylaniline semisquaraine (0.25 g; 1.15 mmol) and *N*-ethyl-2-methyl-1,3-benzothiazole (0.20 g; 1.15 mmol) in a mixture of 2:1 butanol:benzene in the presence of 1 mL of quinoline fitted with a Dean Starck condenser for azeotropic removal of water for about 6 h. After cooling, the reaction mixture was concentrated to 2 mL and precipitated by adding excess hexane. It was then filtered, and the product was purified by column chromatography using silica gel (100–200 mesh) with 1% methanol–chloroform to yield 240 mg (55%) of the pure product.

^{1}H NMR (300 MHz, $CDCl_3$): 8.12–8.15 (d, 2H, J = 8.4 Hz), 7. 72–7. 74 (d, 2H, J = 7.8 Hz), 7.51–7.53 (d, 1H, J = 7.5 Hz), 7.39–7.42 (m,2H), 6.68–6.71 (d, 2H, 8.4 Hz, aromatic), 6.30 (s, 1H, olefinic), 4.37–4.39 (q, 2H, +N–CH_2), 3.07 (s, 6H, $N(CH_3)_2$), 1.48–1.53 (t, 3H) ppm. ^{13}C NMR (125 MHz, $CDCl_3$): 187.24, 181.81, 169.82, 165.21, 152.00, 139.99, 129.90, 129.57, 128.06, 125.99, 122.92, 120.00, 114.07, 112.82, 111.78, 88.76, 42.38, 40.13, 14.12 ppm. FAB-MS: calcd, 376.12; found, 377.60.

RESULTS: ABSORPTION AND EMISSION SPECTRA

Figure 1 shows experimental absorption and emission spectra of asymmetric squaraine dyes D_1–A–D_2 and D_1–A–D_3 collected in a low-polarity solvent, toluene (Tol), and in a strongly polar solvent, acetonitrile (CH_3CN). Spectra collected in solvents of intermediate polarity are reported in Figure S1 in

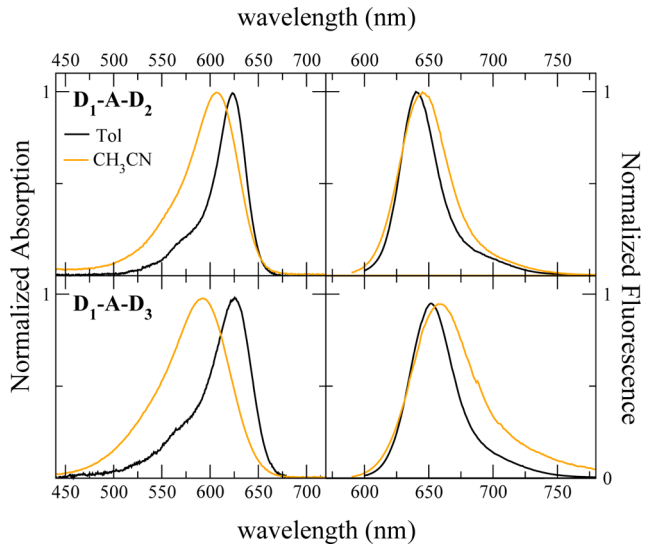

Figure 1. Experimental absorption (left panels) and emission (right panels) spectra of asymmetric dyes D_1–A–D_2 and D_1–A–D_3 collected in solvents of different polarity.

the Supporting Information. Both dyes show strong absorption and emission bands in the red region of the visible spectrum. The bands are fairly narrow in toluene with a weak vibronic shoulder. In acetonitrile the absorption peak is blue shifted with respect to toluene (inverse solvatochromism), while the opposite occurs for emission (normal solvatochromism). As a result, the Stokes shifts, listed in Table 1, considerably increase with solvent polarity. Band shape is also strongly affected: both emission and absorption bands broaden in polar solvents, at variance with symmetric squaraines, whose spectra barely change with solvent. Both D_1–A–D_2 and D_1–A–D_3 are poorly soluble in all solvents, hindering extinction coefficient measurements.

For comparison, Figure 2 shows absorption and emission spectra of the symmetric squaraines D_1–A–D_1 and D_3–A–D_3. Experimental data for D_2–A–D_2, published in ref 51, are not duplicated here. Spectra of symmetric squaraine dyes, very similar to D_2–A–D_2 and D_3–A–D_3, reported in ref 64, are

dx.doi.org/10.1021/jp401099g | J. Phys. Chem. B 2013, 117, 8536–8546

Table 1. Stokes Shifts (in cm^{-1}) Measured for the Molecular Systems Analyzed in Solvents of Different Polarity[a]

	toluene	chloroform	dichloromethane	acetonitrile	DMSO
D_1−A−D_2	426	507	631	971	
D_1−A−D_3	663	752	1023	1717	
D_1−A−D_1	325		468	515	
D_2−A−D_2	215	235			265
D_3−A−D_3	193	243	264		

[a]Data relevant to molecule D_2−A−D_2 are from ref 51. Absorption and emission spectra collected in chloroform and dichloromethane are reported as Supporting Information.

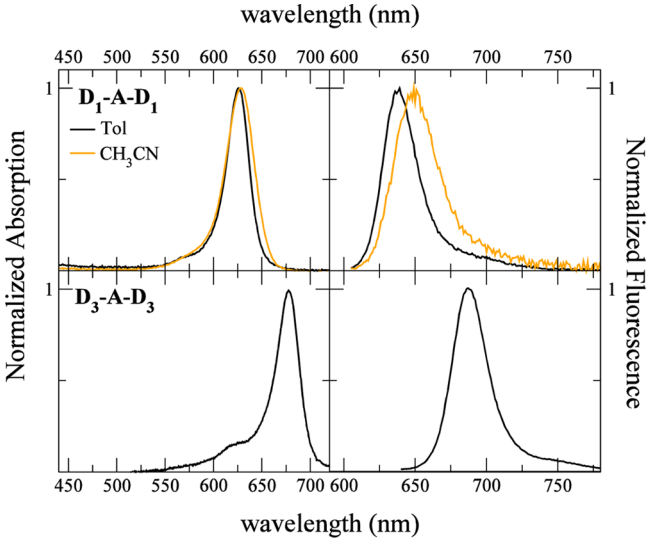

Figure 2. Experimental absorption (left) and emission (right) spectra of symmetric dyes D_1−A−D_1 and D_3−A−D_3 collected in solvents of different polarity. Experimental data for D_2−A−D_2 are available in ref 51.

fully consistent with the present results. Due to aggregation occurring in acetonitrile, spectra of D_3−A−D_3 are only shown in toluene. Symmetric dyes D_1−A−D_1, D_2−A−D_2, and D_3−A−D_3 exhibit the typical behavior of squaraine dyes, with narrow absorption and emission bands, weak vibronic structure, and small Stokes shifts (see Table 1). The dyes are only marginally solvatochromic, and as usual for squaraine dyes, the molar extinction coefficients are very large: 309 000 cm^{-1} M^{-1} for D_1−A−D_1 in dichloromethane[65] and 330 000 cm^{-1} M^{-1} for D_2−A−D_2[51] in toluene (poor solubility of D_3−A−D_3 hindered measurement of its molar extinction coefficient).

RESULTS: ESSENTIAL-STATE MODELING

Linear and nonlinear optical spectra of symmetric squaraines are quantitatively described by essential-state models.[51] A sketch of relevant states is reported in the top panel of Figure 3. The three basis states (the diabatic states on the top left panel) correspond to the three main resonating structures: the neutral structure, N = DAD, and the two zwitterionic structures, Z_L = D^+A^-D and Z_R = DA^-D^+. N is separated by an energy gap 2η from the two mutually degenerate zwitterionic states, Z_R and Z_L, and is mixed to them by a matrix element $-2^{1/2}\tau$. Z_R and Z_L have a large permanent dipole moment, μ_0, with opposite orientation in the two states. The basis is conveniently symmetrized to yield two symmetric states, N and $Z_+ = (Z_L + Z_R)/2^{1/2}$ and an ungerade state $Z_- = (Z_L - Z_R)/2^{1/2}$. The

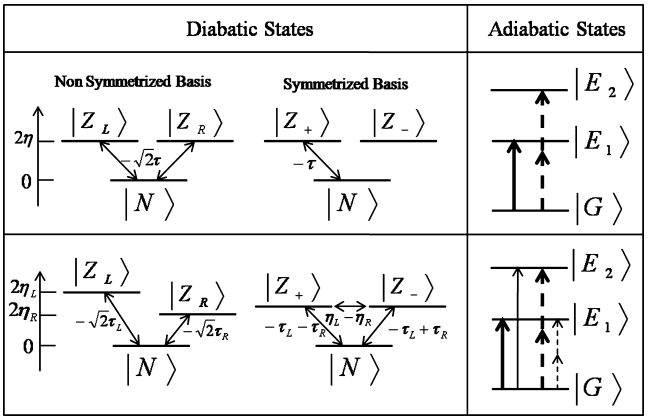

Figure 3. Sketch of essential-state modeling for symmetric (top) and asymmetric squaraine dyes (bottom).

ungerade state Z_- stays unmixed and coincides with the first excited eigenstate, E_1, allowed in 1PA processes. The two gerade states, N and Z_+, mix to yield the ground state, G, and the optically dark eigenstate, E_2, allowed in 2PA. The ground state is characterized by a quadrupolar charge distribution, $D^{+0.5\rho}A^{-\rho}D^{+0.5\rho}$, fully described by a single parameter ρ that measures the weight of Z_+ into the ground state and represents a key quantity for definition of the spectral properties of symmetric quadrupolar dyes.[51]

Optical spectra of asymmetric quadrupolar dyes have already been addressed in refs 66 and 67, but only slightly asymmetric dyes with marginally different donor groups were considered. The dyes discussed here are strongly asymmetric, with different peripheral donor groups and different π bridges, leading to a diverse phenomenology and requiring specific modelization.

The proposed model for asymmetric dyes, sketched in the lower panels of Figure 3, is based on the same three resonance structures N, Z_L, and Z_R adopted for symmetric dyes. However, the two zwitterionic states, Z_L and Z_R, are no longer degenerate but are assigned energies $2\eta_L$ and $2\eta_R$, respectively (cf Figure 3). Moreover, two different mixing matrix elements are defined for the two states: $-2^{1/2}\tau_L = \langle Z_L|H|N\rangle$ and $-2^{1/2}\tau_R = \langle Z_R|H|N\rangle$, and two operators $\hat{\rho}_{L,R} = |Z_{L,R}\rangle\langle Z_{L,R}|$ measure the charge distribution on each molecular arm.

The electronic Hamiltonian and dipole moment operators can be written on the basis of the N, Z_+, and Z_- states as follows

$$H_{el} = \begin{pmatrix} 0 & -\tau_L - \tau_R & -\tau_L + \tau_R \\ -\tau_L - \tau_R & \eta_L + \eta_R & \eta_L - \eta_R \\ -\tau_L + \tau_R & \eta_L - \eta_R & \eta_L + \eta_R \end{pmatrix} \quad (1)$$

$$\hat{\mu} = \frac{1}{2}\begin{pmatrix} 0 & 0 & 0 \\ 0 & (\mu_L - \mu_R) & (\mu_L + \mu_R) \\ 0 & (\mu_L + \mu_R) & (\mu_L - \mu_R) \end{pmatrix} \quad (2)$$

where the L and R indices refer to the left and right molecular arms, respectively. The molecular asymmetry reflects a direct mixing between Z_+ and Z_- (driven by $\eta_L - \eta_R$) and between N and Z_- (driven by $-\tau_L + \tau_R$). The mixing of gerade and ungerade states, made possible by the lack of symmetry, breaks spectroscopic selection rules: the second excited state, E_2, forbidden in 1PA for symmetric dyes, becomes 1PA allowed in

dx.doi.org/10.1021/jp401099g | J. Phys. Chem. B 2013, 117, 8536−8546

asymmetric dyes, while E_1 acquires a sizable 2PA cross-section. Moreover, the permanent dipole moment, strictly vanishing for all states in symmetric dyes, has finite values for all states in asymmetric dyes, in line with the observed solvatochromism.

The discussion of the electronic structure sketched above sets the basis to understand the spectral properties of asymmetric squaraine dyes; however, a complete description of optical spectra, including band shapes and solvent effects, must account for the coupling between electrons and molecular vibrations and polar solvation. Two effective vibrational coordinates, q_L and q_R, are introduced to describe the relaxation of the molecular geometry upon excitation on each molecular arm.[51] The two harmonic coordinates are assigned the frequency $\omega_{L,R}$ and the relaxation energy $\varepsilon_{L,R}$.

As discussed in refs 55−57, the simplest model for solvation describes the solvent as a continuum elastic medium that generates at the solute location an electric field (the so-called reaction field) proportional to the solute dipole moment. Two contributions to the reaction field are conveniently separated, based on the different time scale of the solvent response. The electronic polarization of the solvent occurs on a very fast time scale: the electronic degrees of freedom of solvent molecules (typically in the ultraviolet spectral region) react instantaneously to the CT transition and can be accounted for by a renormalization of model parameters. In the simplest approximation, only the solvent refractive index enters the renormalization and, in view of the marginal variation of the refractive index in common organic solvents, solvent-independent molecular parameters are conveniently assumed.[55−57] In polar solvents the reorientation of the solvent molecules contributes to the reaction field with a very slow motion with respect to the relevant electronic and vibrational degrees of freedom of the solute. To describe this slow motion an effective solvation coordinate is introduced proportional to the orientational component of the reaction field F. This field enters the Hamiltonian as a classical harmonic coordinate whose relaxation energy, ε_{or}, is an effective measure of the solvent polarity.[51,55−57] Indeed, microscopic models have been developed that, assuming a specific shape for the solvent cavity occupied by the solute, relate the solvent relaxation energy to the solvent refractive index and dielectric constant.[55] However, the definition of the shape and size of the solvent cavity introduces large uncertainties in the ε_{or} estimate, so we prefer to consider this parameter as an adjustable model parameter.

With these approximations the total Hamiltonian is

$$H = H_{el} - \sqrt{2\varepsilon_L}\,\omega_L \hat{q}_L \hat{\rho}_L - \sqrt{2\varepsilon_R}\,\omega_R \hat{q}_R \hat{\rho}_R + \frac{1}{2}(\omega_L^2 \hat{q}_L^2 + \omega_R^2 \hat{q}_R^2 + \hat{p}_L^2 + \hat{p}_R^2) - F\hat{\mu} + \frac{F^2}{4\varepsilon_{or}} \quad (3)$$

where the second and third terms account for the coupling between electronic and vibrational degrees of freedom. The fourth term is the Hamiltonian for the two harmonic oscillators q_L and q_R, where p_L and p_R are the corresponding momenta. The last two terms represent the coupling between CT degrees of freedom and polar solvation and the corresponding elastic energy, respectively.

The solvation coordinate is very slow, and its kinetic energy is neglected in the above equation, making F a classical variable that can be treated in the adiabatic approximation. Therefore, the Hamiltonian in eq 3 is diagonalized on a grid of F values to calculate F-dependent eigenstates and eigenvalues. For fixed F, the Hamiltonian describes the coupled motion of electrons and molecular vibrations. We solve this problem in a fully nonadiabatic approach. Specifically, the Hamiltonian is written on the basis obtained as the direct product of the three electronic basis states N, Z_+, and Z_- and the eigenstates of the two harmonic oscillators associated with q_L and q_R. The infinite basis associated with each oscillator is truncated to the first M states, leading to a basis with dimension $3M^2$, where M is large enough to guarantee convergence (M = 10 in this work). Once the nonadiabatic eigenstates are obtained for each F, relevant spectra are calculated according to expressions in ref 68. Solution spectra are finally obtained summing over the spectra calculated for different F values, weighting each spectrum according to the Boltzmann distribution for the ground state (absorption spectra) or for the fluorescent state (emission spectra).

DISCUSSION

As a first step we model optical spectra of the symmetric squaraines, **D$_1$−A−D$_1$**, **D$_2$−A−D$_2$**, and **D$_3$−A−D$_3$**, based on the three-state model for symmetric quadrupolar dyes, as described for **D$_2$−A−D$_2$** in ref 51. Along the same lines, analysis of optical spectra of **D$_1$−A−D$_1$** and **D$_3$−A−D$_3$** in Figure 2 allows for parametrization of the relevant essential-state model, as detailed in Table 2. Calculated spectra in Figure 4 compare well with experiment, giving confidence on the validity of the model. In line with expectation, the parameter η ($= \eta_L = \eta_R$ for symmetric dyes), measuring one-half the energy gap between the zwitterionic states and the neutral state, decreases with increasing the strength of the electron-donor group in the **D$_1$** < **D$_2$** < **D$_3$** series. The parameter τ is responsible for mixing of the basis states and related to the π-conjugated bridge connecting the electron-donor and -acceptor units. Since **D$_2$−A−D$_2$** and **D$_3$−A−D$_3$** have the same π bridge, in order to reduce the number of adjustable parameters, we impose the same τ for both dyes. The vibrational relaxation energy, ε, is estimated for **D$_1$−A−D$_1$** to be smaller than for either **D$_2$−A−D$_2$** or **D$_3$−A−D$_3$**, in line with its more rigid structure. Finally, the effective dipole length μ_0 is fixed for each dye to reproduce the extinction coefficient and shows only marginal variations for the three dyes.

Table 2. Essential-State Parameters Adopted for the Calculation of Spectra in Figures 6 and 7[a]

	D$_1$−A−D$_2$	**D$_1$−A−D$_3$**	**D$_1$−A−D$_1$**	**D$_2$−A−D$_2$**	**D$_3$−A−D$_3$**
η_L (eV)	0.46	0.5	0.45	0.28	0.2
η_R (eV)	0.23	0.12	0.45	0.28	0.2
$2^{1/2}\tau_L$ (eV)	1.05	1.05	1.05	1.2	1.2
$2^{1/2}\tau_R$ (eV)	1.2	1.2	1.05	1.2	1.2
μ_L(D)	22	22	22	21	18
μ_R (D)	21	18	22	21	18
ε_L (eV)	0.05	0.05	0.05	0.16	0.16
ε_R (eV)	0.16	0.16	0.05	0.16	0.16
ω_L (eV)	0.15	0.15	0.15	0.16	0.15
ω_R (eV)	0.16	0.15	0.15	0.16	0.15

[a]Intrinsic line width of each vibronic transition (HWHM) Γ is set to 0.05 eV for all molecules. Parameters for **D$_2$−A−D$_2$** are taken from ref 51. For the three symmetric dyes the right and left arm of the molecule are equivalent so that relevant parameters are equal.

Having extracted a reliable set of model parameters for symmetric dyes, we are now in the position to discuss

dx.doi.org/10.1021/jp401099g | J. Phys. Chem. B 2013, 117, 8536−8546

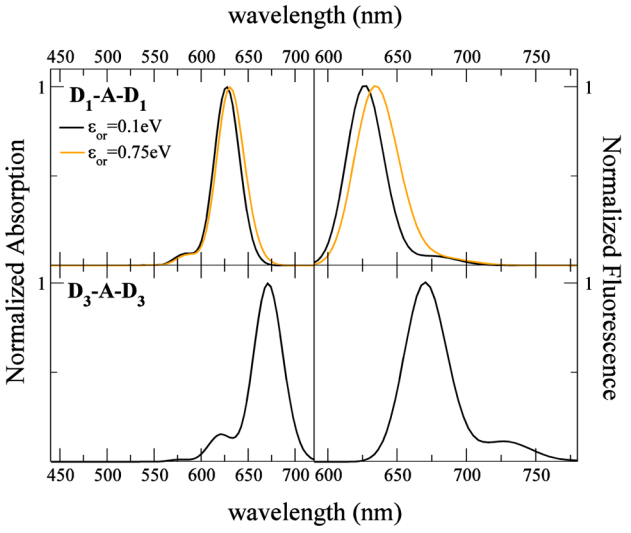

Figure 4. Calculated absorption (left) and emission (right) spectra of dyes $\mathbf{D_1}$–$\mathbf{A}$–$\mathbf{D_1}$ and $\mathbf{D_3}$–$\mathbf{A}$–$\mathbf{D_3}$. Model parameters are reported in Table 2. Calculated spectra of $\mathbf{D_2}$–$\mathbf{A}$–$\mathbf{D_2}$ can be found in ref 51.

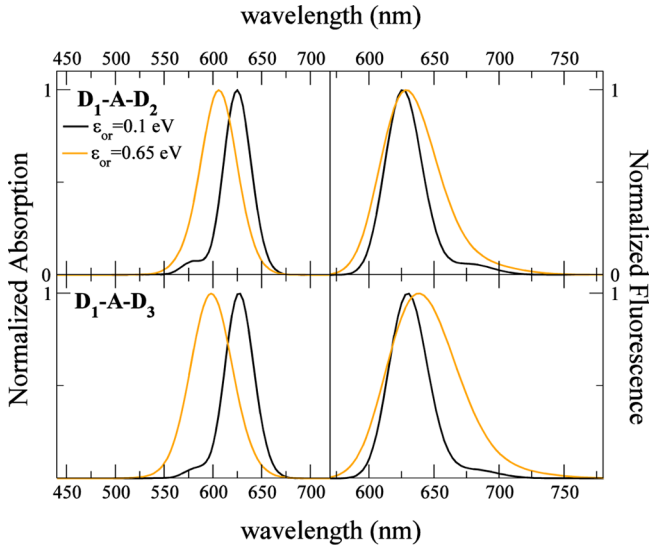

Figure 5. Calculated absorption (left) and emission (right) spectra of asymmetric squaraine dyes $\mathbf{D_1}$–$\mathbf{A}$–$\mathbf{D_2}$ and $\mathbf{D_1}$–$\mathbf{A}$–$\mathbf{D_3}$. Model parameters are listed in Table 2.

asymmetric squaraines. All model parameters of symmetric dyes are rigidly transferred to model asymmetric dyes, as shown in Table 2, with the notable exception of η_L and η_R that are tuned to best reproduce experimental optical spectra in Figure 1. In fact η_L, measuring one-half the energy required to move an electron from the left-side group toward the central acceptor group, depends on the relative strength of the involved donor and acceptor groups: η_L is therefore affected by the nature of the D_R donor group that, attached to the central acceptor group, affects its strength (the same of course holds true for η_R that is affected by the nature of D_L). The acceptor strength of the central core decreases when connected to stronger donors ($\mathbf{D_2}$, $\mathbf{D_3}$), and the $\eta_{L,R}$ value associated to the weaker donor increases in the asymmetric molecules, the opposite being true for the $\eta_{R,L}$ value associated to the stronger donor that further decreases. Specifically, in the symmetric molecule $\mathbf{D_1}$–$\mathbf{A}$–$\mathbf{D_1}$ ($\mathbf{D_1}$ is a weaker electron-donor group with respect to $\mathbf{D_2}$ and $\mathbf{D_3}$) $\eta_L = \eta_R = 0.45$ eV. The value of η_L in the asymmetric molecules increases to 0.46 and 0.5 eV in $\mathbf{D_1}$–$\mathbf{A}$–$\mathbf{D_2}$ and $\mathbf{D_1}$–$\mathbf{A}$–$\mathbf{D_3}$, respectively. At the same time η_R decreases from 0.28 to 0.23 eV for $\mathbf{D_2}$ and from 0.2 to 0.12 eV for $\mathbf{D_3}$. As expected, the variation of $\eta_{L,R}$ values is more pronounced as the difference of the electron-donor strength of the two peripheral groups increases.

Figure 5 shows calculated absorption and emission spectra for asymmetric dyes, to be compared with experimental data in Figure 1. The three-state model proposed for asymmetric quadrupolar dyes reproduces accurately the opposite solvatochromism observed for absorption and fluorescence as well as the pronounced spectral broadening in polar solvents. The model does not account for the small Stokes shift observed in low-polarity solvent. The coupling to a slow conformational degree of freedom[69,70] could easily correct this minor effect.

To better understand the physical origin of the spectroscopic behavior of asymmetric squaraines, Figure 6 shows the potential energy surfaces (PES, energy as a function of the reaction field) for the ground and fluorescent states, calculated for $\mathbf{D_1}$–$\mathbf{A}$–$\mathbf{D_3}$ in toluene and acetonitrile (top and bottom panels, respectively; similar PES calculated for $\mathbf{D_1}$–$\mathbf{A}$–$\mathbf{D_2}$ can be found in the Supporting Information). Left panels refer to

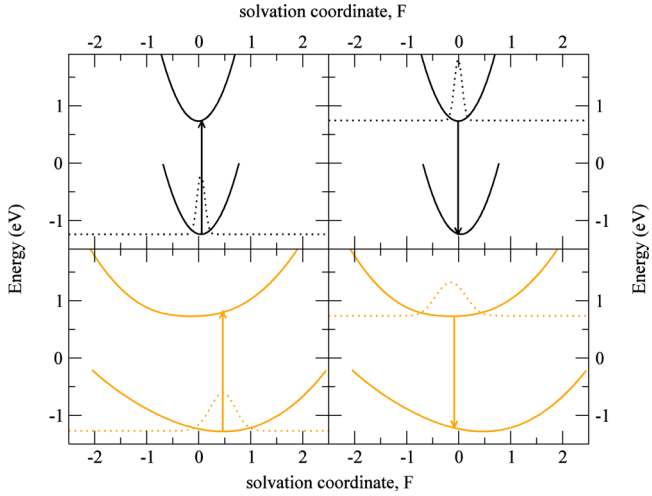

Figure 6. Energy of the ground and fluorescent state (potential energy surfaces, continuous lines) plotted versus the orientational reaction field. Results in the top and bottom panels refer to $\mathbf{D_1}$–$\mathbf{A}$–$\mathbf{D_3}$ in toluene (black ε_{or} = 0.1 eV) and acetonitrile (orange ε_{or} = 0.65 eV), respectively. In the left panels, arrows refer to the absorption process and dotted lines show the ground-state Boltzmann distribution. In the right panels, arrows refer to the emission process and dotted lines show the Boltzmann distribution for the fluorescent state. For graphical reasons the distributions are arbitrarily normalized to an area that for the most polar solvent is twice as the area for the less polar solvents.

the absorption process; accordingly, the dotted line in this panel shows the calculated Boltzmann distribution based on the ground-state energy. Right panels instead refer to fluorescence, and the dotted line shows in this case the Boltzmann distribution calculated for the emitting state. In the weakly polar solvent (top panels) the minima of both the ground- and the excited-state PES, and hence the maxima of the relevant Boltzmann distributions, are centered approximately at $F = 0$, pointing to small permanent dipole moments for both states. This explains the negligible Stokes shift and the narrow band shapes calculated in low-polarity solvents. On the other hand,

dx.doi.org/10.1021/jp401099g | J. Phys. Chem. B 2013, 117, 8536–8546

in a strongly polar solvent (bottom panels of Figure 6) the ground-state PES is clearly shifted toward positive F while the PES relevant to the first excited state is slightly shifted toward negative F values, suggesting an opposite orientation of the ground- and excited-state permanent dipole moments, as will be discussed below. As a result, upon increasing solvent polarity the absorption moves to higher frequency (the orange arrow is longer than the black arrow in the left panels of Figure 6), but the opposite is true for fluorescence (the orange arrow is shorter than the black arrow in the right panels). The broadening of both absorption and fluorescence bands is explained by the broad Boltzmann distribution calculated in polar solvents spanning a sizable range of values of transition frequencies.

For comparison, the PESs calculated for the symmetric dye $\mathbf{D_1}$−$\mathbf{A}$−$\mathbf{D_1}$ are reported in Figure 7: in contrast with

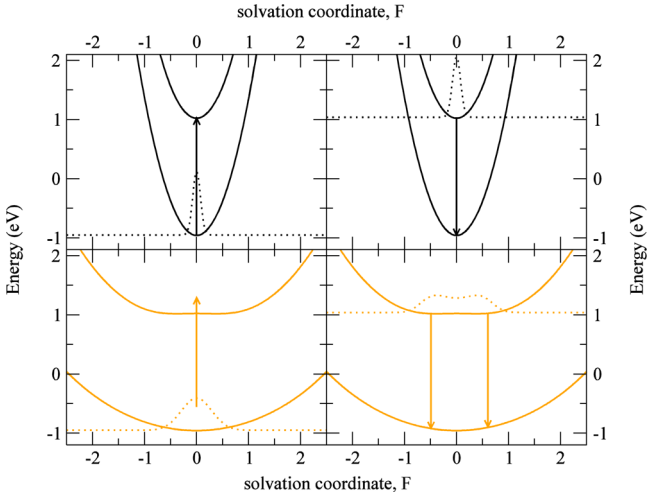

Figure 7. Same as Figure 6 but for the symmetric $\mathbf{D_1}$−$\mathbf{A}$−$\mathbf{D_1}$ dye. Top and bottom panels show results obtained for ε_{or} = 0.1 (as relevant to toluene) and 0.75 eV (acetonitrile).

asymmetric molecules, the minimum of the PES is located at F = 0, with the exception of the excited-state PES in polar solvent that shows a very shallow double minimum, suggesting incipient symmetry breaking in the fluorescent state, and locating $\mathbf{D_1}$−$\mathbf{A}$−$\mathbf{D_1}$ at the borderline between class I and class II quadrupolar dyes.[51] Absorption is clearly nonsolvatochromic, while the weak red shift of the emission observed in polar solvent can be attributed to symmetry breaking in the excited state. Moreover, since in each solvent the ground and excited PES are centered at the same F and have similar curvature, the F dependence of the transition frequency is very weak, leading to largely reduced spectral broadening with respect to asymmetric dyes.

The incipient symmetry breaking observed for $\mathbf{D_1}$−$\mathbf{A}$−$\mathbf{D_1}$ in strongly polar solvents locates this dye at the borderline between class II and class I in our classification of quadrupolar chromophores.[51] This behavior is related to the comparatively poor electron-donating character of $\mathbf{D_1}$ with respect to $\mathbf{D_2}$ and $\mathbf{D_3}$, leading to a larger η value and comparatively lower ρ. PES calculated for $\mathbf{D_2}$−$\mathbf{A}$−$\mathbf{D_2}$ and $\mathbf{D_3}$−$\mathbf{A}$−$\mathbf{D_3}$ do not support symmetry breaking (see Figures S4 and S5 in the Supporting Information), and these squaraines can then be classified as pure class II quadrupolar dyes with nonsolvatochromic absorption and fluorescence.[51] Indeed, experimental spectra of $\mathbf{D_2}$−$\mathbf{A}$−$\mathbf{D_2}$ show a marginal solvatochromism which is most probably related to specific solute−solvent interactions (it is in fact more pronounced for chlorinated solvents) and/or to the neglected effects of the variation of the solute refractive index.

Once parametrized against linear absorption and fluorescence spectra, essential-state models can be used to predict other spectral properties. Figures S6 and S7 in the Supporting Information show calculated two-photon absorption (2PA) and hyper-Rayleigh scattering (HRS) spectra of the different compounds. As is often the case for squaraine dyes, the very intense 2PA band associated with the E_2 state corresponds to a state with a similar energy as twice the energy of the linear absorption. In this condition one-photon absorption processes mask 2PA processes, making measurement and/or calculation of 2PA spectra impossible. The lowest electronic excited state is nominally 2PA forbidden in symmetric squaraines. Indeed, it acquires a low intensity mainly due to inhomogeneous broadening effects in polar solvents. As shown for $\mathbf{D_1}$−$\mathbf{A}$−$\mathbf{D_1}$ in the left panels of Figure 6, states with finite F, corresponding to states with a lowered symmetry, are thermally populated in polar solvents. Accordingly, the 2PA intensity calculated for the symmetric dye is negligible for ε_{or} = 0.1 eV but becomes sizable for ε_{or} = 0.65 eV. Similarly, one expects vanishing HRS signals for centrosymmetric molecules, and in fact, the calculated response (β_{HRS}) vanishes in nonpolar (ε_{or} = 0) solvents for symmetric squaraines, but sizable signals are observed in polar solvents (ε_{or} ≠0). Of course, nonsymmetric squaraines show sizable 2PA intensity in the 1PA region and finite HRS intensity already in nonpolar solvents, and for these molecules the effects of solvent polarity on nonlinear responses are marginal.

We now discuss the charge distribution on asymmetric squaraines both in the ground and in the fluorescent states, an important issue to understand their anomalous solvatochromism as well as for applicative purposes. Since the molecule is overall neutral, the charge distribution is fully defined by ρ_L and ρ_R, the expectation values of the operators $\hat{\rho}_L$ and $\hat{\rho}_R$ defined above. The total charge on the central acceptor is $-\rho = -(\rho_L + \rho_R)$. The quantity ρ is therefore proportional to the molecular quadrupole moment and has exactly the same meaning as in the standard model for symmetric quadrupolar dyes.[51] The evolution with ε_{or} of ρ calculated for the ground and fluorescent states of $\mathbf{D_1}$−$\mathbf{A}$−$\mathbf{D_2}$ is plotted in the top panel of Figure 8 (similar results for $\mathbf{D_1}$−$\mathbf{A}$−$\mathbf{D_3}$ are shown in Figure S8 in the Supporting Information). The bottom panel in the same figure shows the charge difference $\rho_L - \rho_R$. This quantity, strictly

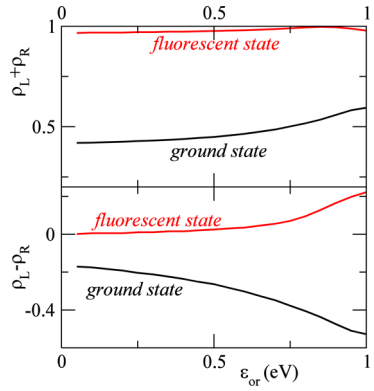

Figure 8. Calculated charge distribution for the ground and excited states of $\mathbf{D_1}$−$\mathbf{A}$−$\mathbf{D_2}$. (Top and bottom) $\rho_L + \rho_R$ and $\rho_L - \rho_R$, respectively, plotted as a function of the solvent relaxation energy, ε_{or}.

dx.doi.org/10.1021/jp401099g | J. Phys. Chem. B 2013, 117, 8536−8546

vanishing in symmetric quadrupolar dyes, is related to the molecular dipole moment. In polar solvents, the reaction field couples with the molecular dipole moment rather than the quadrupole moment. Indeed $\rho_L + \rho_R$ is only marginally affected by the solvent polarity: in the ground state it shows just a minor increase with ε_{or}, while in the excited state $\rho_L + \rho_R$ is always very close to the limiting value of 1, expected for symmetric dyes.[51] More interesting is the $\rho_L - \rho_R$ behavior: polar solvents favor polar states, and the absolute value of $\rho_L - \rho_R$ increases with ε_{or}. Interestingly, in the ground state $\rho_L - \rho_R$ is negative: the charge on the weaker donor site on the left side is smaller than the charge on the right side, corresponding to the stronger donor, and the charge unbalance increases with solvent polarity. In the excited state however the sign of $\rho_L - \rho_R$ is positive: depletion of charge is larger for the weakest than for the strongest donor. This inversion of course corresponds to an inverted direction of the molecular dipole moment from the ground to the fluorescent state. Solvatochromic shifts in absorption and emission are proportional to $\mu_G(\mu_E - \mu_G)$ and $\mu_E(\mu_E - \mu_G)$, respectively:[71,72] $\mu_G(\mu_E - \mu_G)$ is clearly negative (both μ_E and $-\mu_G$ have opposite direction than μ_G), in line with the inverse solvatochromism observed for absorption, but $\mu_E(\mu_E - \mu_G)$ is positive (μ_E and $-\mu_G$ both point in the same direction as μ_E), supporting normal solvatochromism for fluorescence. Moreover, since $\mu_E < \mu_G$, a weaker solvatochromism is expected in emission than in absorption.

Asymmetric squaraine dyes are actively investigated as light-absorbing species in unconventional photovoltaic (OPV and DSSC) applications.[30−40] In both cases squaraine dyes are useful due to their intense absorption in the visible spectral region. Asymmetric squaraines are more promising than their symmetric counterparts mainly because of the possibility to tune their absorption frequency as to better match (particularly with blends of several dyes) the solar spectrum, as well as for the overall broader absorption features. Both in OPV and in DSSC devices the excited dyes must inject an electron toward an acceptor, usually a C_{60} or a C_{60} derivative in OPV or a nanostructured semiconductor (typically titania nanoparticles) in DSSC. Charge injection is therefore favored if the asymmetric squaraine *in the excited state* has a lateral site (one of the two donor sites) that is comparatively electron rich and if this site is located near the electron accepting species. More specifically, in DSSC it is important to design the asymmetric squaraine dye as to have the donor site richer in electrons in the excited state directly attached to the nanostructured semiconductor as to favor charge injection upon photoexcitation.

Figure 9 shows ρ_L and ρ_R calculated as a function of ε_{or} for $\mathbf{D_1}$−$\mathbf{A}$−$\mathbf{D_2}$ (similar results for $\mathbf{D_1}$−$\mathbf{A}$−$\mathbf{D_3}$ are reported in Figure S9 in the Supporting Information). As discussed above, in the ground state the left site, corresponding to the weaker donor, is more electron rich than the right site (as expected on physical basis), but the opposite is true for the excited state (bottom panel of Figure 9), suggesting that for improved efficiency the asymmetric squaraine dye should be attached to the semiconductor through the strong donor site that, in the excited state, is expected to have a larger electron density than the weak donor site. This counterintuitive result was obtained, allowing the solvent to relax following photoexcitation in response to the charge distribution in the excited state, and it is therefore relevant to low-viscosity (liquid) solvents or in any case to systems where electron transfer from the dye to the acceptor species occurs on a slower time scale than the reorientation of

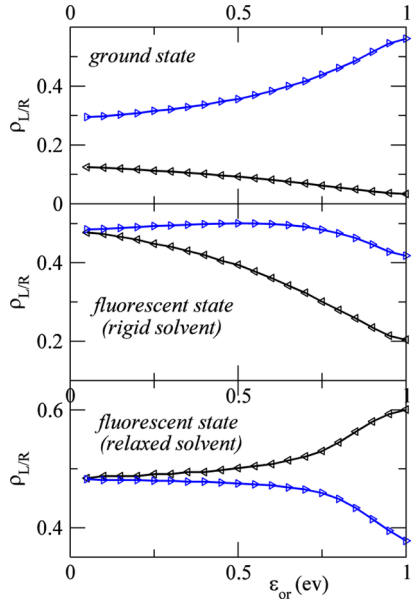

Figure 9. ρ_L (black, left triangles) and ρ_R (blue, right triangles) calculated as a function of ε_{or} for $\mathbf{D_1}$−$\mathbf{A}$−$\mathbf{D_2}$: (top) ground state; (middle) fluorescent state in a rigid solvent; (bottom) fluorescent state in a liquid solvent.

polar solvent molecules (typically in the 1−10 ps time scale, depending on the solvent). In highly viscous or rigid matrices, the solvent cannot relax after photoexcitation and the reaction field stays fixed to the ground-state value. To simulate a rigid environment we suppress the solvent relaxation while allowing the much faster (typically 100 fs) relaxation of molecular geometry upon excitation. The calculated charge distribution in the excited state in a rigid environment is very different from that calculated for a liquid environment: from the results in the central panel of Figure 9, it turns out that in a rigid matrix the donor site richer in electron is the one corresponding to the weaker donor, much as it occurs in the ground state. Either in liquid solvents or in rigid matrix, the best results are expected in strongly polar media, with the rigid medium leading to the most favorable result (smallest ρ values on one of the two donor sites).

■ CONCLUSIONS

Two asymmetric squaraine dyes and their parent symmetric analogues have been synthesized and fully characterized spectroscopically, offering a safe base for definition of quantitative essential-state models for this interesting class of molecules. The developed model fully rationalizes the observed spectral features in terms of band positions, shapes, and intensities. Of particular interest is the rationalization of anomalous solvatochromism shown by asymmetric squaraines, in particular, the inverse solvatochromism of the absorption band and the normal solvatochromism of the fluorescence band which is related to inversion of the permanent molecular dipole moment when going from the ground to the fluorescent state. The fluorescent state, corresponding to the lowest excited electronic state, is the same state involved in electron-injection processes in either DSSC or OPV devices. Inversion of the permanent dipole moment from the ground to the excited state then implies a reversed charge distribution on the two lateral D sites, with the stronger donor, being less rich in electrons in the ground state, becoming more electron rich in the excited state.

dx.doi.org/10.1021/jp401099g | J. Phys. Chem. B 2013, 117, 8536−8546

This has obvious important consequences in optimal design of solar cells. However, the charge redistribution upon photoexcitation is extremely sensitive to the local environment: it depends not only on the solvent polarity but also on the nature of the solvent and its viscosity. The dipole moment inversion is in fact expected for the two investigated asymmetric squaraines only in liquid polar solvents. In viscous polar solvents (like, e.g., in solid solutions or polymers) the dipole moment inversion upon photoexcitation is not expected. The details of the charge distribution in the fluorescent state are obviously important for optimal design of solar cells and strongly affected by the local environment: based on the proposed essential-state models, detailed analysis of the solvatochromism of asymmetric squaraine dyes offers reliable information on this critical issue.

■ ASSOCIATED CONTENT

Supporting Information

Spectra of $\mathbf{D_1-A-D_2}$, $\mathbf{D_1-A-D_3}$, $\mathbf{D_1-A-D_1}$, and $\mathbf{D_3-A-D_3}$ collected in solvents of different polarity; calculated potential energy surfaces for $\mathbf{D_1-A-D_2}$, $\mathbf{D_2-A-D_2}$, and $\mathbf{D_3-A-D_3}$; calculated two-photon absorption and hyper-Rayleigh scattering spectra; calculated charge distribution for the ground and excited states of $\mathbf{D_1-A-D_3}$; calculated ρ_L and ρ_R for $\mathbf{D_1-A-D_3}$. This material is available free of charge via the Internet at http://pubs.acs.org.

■ AUTHOR INFORMATION

Corresponding Author

*E-mail: cristina.sissa@unipr.it.

Notes

The authors declare no competing financial interest.

■ ACKNOWLEDGMENTS

Research grants from the Department of Science and Technology (DST), India, and the Indo- European collaborative project, OISC-LARGECELLS, are gratefully acknowledged. S.K.M. thanks UGC, Government of India for a research fellowship. C.S. thanks the University of Parma and the Italian Ministry of University and Research (MIUR) for financial support through the Project FIRB-Futuro in Ricerca RBFR10Y5VW.

■ REFERENCES

(1) Yamashita, Y. Organic Semiconductors for Organic Field-Effect Transistors. *Sci. Technol. Adv. Mater.* **2009**, *10*, 024313.

(2) Allard, S.; Forster, M.; Souharce, B.; Thiem, H.; Scherf, U. Organic Semiconductors for Solution-Processable Field-Effect Transistors (OFETs). *Angew. Chem., Int. Ed.* **2008**, *47*, 4070−4098.

(3) Coropceanu, V.; Cornil, J.; Da Silva Filho, D. A.; Olivier, Y.; Silbey, R.; Bredas, J.-L. Charge Transport in Organic Semiconductors. *Chem. Rev.* **2007**, *107*, 926−952.

(4) Hagfeldt, A.; Boschloo, G.; Sun, L.; Kloo, L.; Pettersson, H. Dye-Sensitized Solar Cells. *Chem. Rev.* **2010**, *110*, 6595−6663.

(5) Li, Y.; Guo, Q.; Li, Z.; Pei, J.; Tian, W. Solution Processable D-A Small Molecules for Bulk-Heterojunction Solar Cells. *Energy Environ. Sci.* **2010**, *3*, 1427−1436.

(6) Shirota, Y.; Kageyama, H. Charge Carrier Transporting Molecular Materials and Their Applications in Devices. *Chem. Rev.* **2007**, *107*, 953−1010.

(7) Law, K. Y. Organic Photoconductive materials: recent trends and developments. *Chem. Rev.* **1993**, *93*, 449−486.

(8) Das, S.; Thomas, K. G.; George, M. V. In *Organic photochemistry*; Ramamurthy, V., Schanze, K. S., Eds.; Marcel Decker, Inc.: New York; 1997; Vol. *1*, pp 467−517.

(9) Ramaiah, D.; Joy, A.; Chandrasekhar, N.; Eldho, N. V.; Das, S.; George, M. V. Halogenated Squaraine Dyes as Potential Photochemotherapeutic Agents. Synthesis and Study of Photophysical Properties and Quantum Efficiencies of Singlet Oxygen Generation. *Photochem. Photobiol.* **1997**, *65*, 783−790.

(10) Ajayaghosh, A. Chemistry of Squaraine-Derived Materials: Near-IR Dyes, Low Band Gap Systems, and Cation Sensors. *Acc. Chem. Res.* **2005**, *38*, 449−459.

(11) Sreejith, S.; Carol, P.; Chithra, P.; Ajayaghosh, A. Squaraine Dyes: A Mine of Molecular Materials. *J. Mater. Chem.* **2008**, *18*, 264−274.

(12) Beverina, L.; Salice, P. Squaraine Compounds: Tailored Design and Synthesis towards a Variety of Material Science Applications. *Eur. J. Org. Chem.* **2010**, *2010*, 1207−1225.

(13) Wojcik, A.; Nicolaescu, R.; Kamat, P. V.; Chandrasekaran, Y.; Patil, S. Photochemistry of Far Red Responsive Tetrahydroquinoxaline-Based Squaraine Dyes. *J. Phys. Chem. A* **2010**, *114*, 2744−2750.

(14) Dirk, C. W.; Cheng, L.-T.; Kuzyk, M. G. A Simplified Three-Level Model Describing the Molecular Third-Order Nonlinear Optical Susceptibility. *Int. J. Quantum Chem.* **1992**, *43*, 27−36.

(15) Yu, Y. Z.; Shi, R. F.; Garito, A. F.; Grossman, C. H. Origin of Negative $\chi(3)$ in Squaraines: Experimental Observation of Two-Photon States. *Opt. Lett.* **1994**, *94*, 786−788.

(16) Chen, C. T.; Marder, S. R.; Cheng, L. T. Syntheses and Linear and Nonlinear Optical Properties of Unsymmetrical Squaraines with Extended Conjugation. *J. Am. Chem. Soc.* **1994**, *116*, 3117−3118.

(17) Scherer, D.; Dörfler, R.; Feldner, A.; Vogtmann, T.; Schwoerer, M.; Lawrentz, U.; Grahn, W.; Lambert, C. Two-Photon States in Squaraine Monomers and Oligomers. *Chem. Phys.* **2002**, *279*, 179−207.

(18) Chung, S.-J.; Zheng, S.; Odani, T.; Beverina, L.; Fu, J.; Padilha, L. A.; Biesso, A.; Hales, J. M.; Zhan, X.; Schmidt, K.; et al. Extended Squaraine Dyes with Large Two-Photon Absorption Cross-Sections. *J. Am. Chem. Soc.* **2006**, *128*, 14444−14445.

(19) Fu, J.; Padilha, A.; Hagan, D. J.; Van Stryland, E. W.; Przhonska, O. V.; Bondar, M. V.; Slominsky, Y. L.; Kachkovski, A. D. Experimental and Theoretical Approaches to Understanding Two-Photon Absorption Spectra in Polymethine and Squaraine Molecules. *J. Opt. Soc. Am. B* **2007**, *24*, 67−76.

(20) Beverina, L.; Crippa, M.; Landenna, M.; Ruffo, R.; Salice, P.; Silvestri, F.; Versari, S.; Villa, A.; Ciaffoni, L.; Collini, E.; et al. Assessment of Water-Soluble π-Extended Squaraines as One- and Two-Photon Singlet Oxygen Photosensitizers: Design, Synthesis, and Characterization. *J. Am. Chem. Soc.* **2008**, *130*, 1894−1902.

(21) Prabhakar, C.; Bhanuprakash, K.; Rao, V. J.; Balamuralikrishna, M.; Rao, D. N. Third Order Nonlinear Optical Properties of Squaraine Dyes Having Absorption below 500 nm: A Combined Experimental and Theoretical Investigation of Closed Shell Oxyallyl Derivatives. *J. Phys. Chem. C* **2010**, *114*, 6077−6089.

(22) Lee, Y. D.; Lim, C. K.; Kim, S.; Kwon, I. C.; Kim, J. Squaraine-Doped Functional Nanoprobes: Lipophilically Protected Near-Infrared Fluorescence for Bioimaging. *Adv. Funct. Mater.* **2010**, *20*, 2786−2793.

(23) Collini, E.; Carlotto, S.; Ferrante, C.; Bozio, R.; Polimeno, A.; Bloino, J.; Barone, V.; Ronchi, E.; Beverina, L.; Pagani, G. A. Multipolar Symmetric Squaraines with Large Two-Photon Absorption Cross-Sections in the NIR Region. *Phys. Chem. Chem. Phys.* **2011**, *13*, 12087−12094.

(24) Avirah, R. R.; Jayaram, D. T.; Adarsh, N.; Ramaiah, D. Squaraine Dyes in PDT: from Basic Design to *In Vivo* Demonstration. *Org. Biomol. Chem.* **2012**, *10*, 911−920.

(25) Silvestri, F.; Irwin, M. D.; Beverina, L.; Facchetti, A.; Pagani, G. A.; Marks, T. J. Efficient Squaraine-Based Solution Processable Bulk-Heterojunction Solar Cells. *J. Am. Chem. Soc.* **2008**, *130*, 17640−17641.

(26) Mayerhoffer, U.; Deing, K.; Gruss, K.; Braunschweig, H.; Meerholz, K.; Wurthner, F. Outstanding Short-Circuit Currents in BHJ Solar CellsBased on NIR-Absorbing Acceptor-Substituted Squaraines. *Angew. Chem., Int. Ed.* **2009**, *48*, 8776−8779.

(27) Silvestri, F.; Lopez-Duarte, I.; Seitz, W.; Beverina, L.; Martinez-Diaz, M. V.; Marks, T. J.; Guldi, D. M.; Pagani, G. A.; Torres, T. A squaraine−phthalocyanine ensemble: towards molecular panchromatic sensitizers in solar cells. *Chem. Commun.* **2009**, 4500−4502.
(28) Bagnis, D.; Beverina, L.; Huang, H.; Silvestri, F.; Yao, Y.; Yan, H.; Pagani, G. A.; Marks, T. J.; Facchetti, A. Marked Alkyl- vs Alkenyl-Substitutent Effects on Squaraine Dye Solid-State Structure, Carrier Mobility, and Bulk-Heterojunction Solar Cell Efficiency. *J. Am. Chem. Soc.* **2010**, *132*, 4074−4075.
(29) Völker, S. F.; Uemura, S.; Limpinsel, M.; Mingebach, M.; Deibel, C.; Dyakonov, V.; Lambert, C. Polymeric Squaraine Dyes as Electron Donors in Bulk Heterojunction Solar Cells. *Macromol. Chem. Phys.* **2010**, *211*, 1098−1108.
(30) Wang, S.; Hall, L.; Diev, V. V.; Haiges, R.; Wei, G.; Xiao, X.; Djurovich, P. I.; Forrest, S. R.; Thompson., M. E. N,N-Diarylanilinosquaraines and Their Application to Organic Photovoltaics. *Chem. Mater.* **2011**, *23*, 4789−4798.
(31) Wei, G.; Wang, S.; Renshaw, K.; Thompson, M. E.; Forrest, S. R. Solution-Processed Squaraine Bulk Heterojunction Photovoltaic Cells. *ACS Nano* **2010**, *4*, 1927−1934.
(32) Wei, G.; Lunt, R. R.; Sun, K.; Wang, S.; Thompson, M. E.; Forrest, S. R. Efficient, Ordered Bulk Heterojunction Nanocrystalline Solar Cells by Annealing of Ultrathin Squaraine Thin Films. *Nano Lett.* **2010**, *10*, 3555−3559.
(33) Alex, S.; Santhosh, U.; Das, S. Dye sensitization of nanocrystalline TiO2: enhanced efficiency of unsymmetrical versus symmetrical squaraine dyes. *J. Photochem. Photobiol. A* **2005**, *172*, 63−71.
(34) Otsuka, A.; Funabiki, K.; Sugiyama, N.; Yoshida, T. Dye Sensitization of ZnO by Unsymmetrical Squaraine Dyes Suppressing Aggregation. *Chem. Lett.* **2006**, *35*, 666−667.
(35) Yum, J. H.; Walter, P.; Huber, S.; Rentsch, D.; Geiger, T.; Nuesch, F.; De Angelis, F.; Gratzel, M.; Nazeeruddin, M. K. Efficient Far Red Sensitization of Nanocrystalline TiO2 Films by an Unsymmetrical Squaraine Dye. *J. Am. Chem. Soc.* **2007**, *129*, 10320−10321.
(36) Geiger, T.; Kuster, S.; Yum, J. H.; Moon, S. J.; Nazeeruddin, M. K.; Gratzel, M.; Nuesch, F. Molecular Design of Unsymmetrical Squaraine Dyes for High Efficiency Conversion of Low Energy Photons into Electrons Using TiO_2 Nanocrystalline Films. *Adv. Funct. Mater.* **2009**, *19*, 2720−2727.
(37) Shi, Y.; Hill, R. B. M.; Yum, J.-H.; Dualeh, A.; Barlow, S.; Graetzel, M.; Marder, S. R.; Nazeeruddin, M. K. A High-Efficiency Panchromatic Squaraine Sensitizer for Dye-Sensitized Solar Cells. *Angew. Chem., Int. Ed.* **2011**, *50*, 6619−6621.
(38) Paek, S.; Choi, H.; Kim, C.; Cho, N.; So, S.; Song, K.; Nazeeruddin, M. K.; Ko, J. Efficient and Stable Panchromatic Squaraine Dyes for Dye-Sensitized Solar Cells. *Chem. Commun.* **2011**, *47*, 2874−2876.
(39) Beverina, L.; Ruffo, R.; Mari, C. M.; Pagani, G. A.; Sassi, M.; De Angelis, F.; Fantacci, S.; Yum, J.-H.; Gratzel, M.; Nazeeruddin, M. K. Panchromatic Cross-Substituted Squaraines for Dye-Sensitized Solar Cell Applications. *ChemSusChem* **2009**, *2*, 621−624.
(40) Li, J.-Y.; Chen, C.-Y.; Lee, C.-P.; Chen, S.-C.; Lin, T.-H.; Tsai, H.-H.; Ho, K.-C.; Wu, C.-G. Unsymmetrical Squaraines Incorporating the Thiophene Unit for Panchromatic Dye-Sensitized Solar Cells. *Org. Lett.* **2010**, *12*, 5454−5457.
(41) Welder, F.; Paul, B.; Nakazumi, H.; Yagi, S.; Colyer, C. L. Symmetric and Asymmetric Squarylium Dyes as Noncovalent Protein Labels: a Study by Fluorimetry and Capillary Electrophoresis. *J. Chromatogr. B* **2003**, *793*, 93−105.
(42) Basheer, M. C.; Alex, S.; Thomas, K. G.; Suresh, C. H.; Das, S. A squaraine-based chemosensor for Hg^{2+} and Pb^{2+}. *Tetrahedron* **2006**, *62*, 605−610.
(43) Chen, C.; Dong, H.; Chen, Y.; Guo, L.; Wang, Z.; Sun, J.-J.; Fu, N. Dual-Mode Unsymmetrical Squaraine-Based Sensor for Selective Detection of Hg^{2+} in Aqueous Media. *Org. Biomol. Chem.* **2011**, *9*, 8195−8201.
(44) Luo, C.; Zhou, Q.; Lei, W.; Wang, J.; Zhang, B.; Wang, X. Supramolecular Assembly of a New Squaraine and β-Cyclodextrin for Detection of Thiol-Containing Amino Acids in Water. *Supramol. Chem.* **2011**, *23*, 657−662.
(45) Shafeekh, K. M.; Rahim, M. K. A.; Basheer, M. C.; Suresh, C. H.; Das, S. Highly Selective and Sensitive Colourimetric Detection of Hg^{2+} Ions by Unsymmetrical Squaraine Dyes. *Dyes Pigm.* **2013**, *96*, 714−721.
(46) Meyers, F.; Chen, C. T.; Marder, S. R.; Bredas, J.-L. Electronic Structure and Linear and Nonlinear Optical Properties of Symmetrical and Unsymmetrical Squaraine Dyes. *Chem.—Eur. J.* **1997**, *3*, 530−537.
(47) Prabhakar, Ch.; Yesudas, K.; Krishna Chaitanya, G.; Sitha, S.; Bhanuprakash, K.; Jayathirtha Rao, V. Near-Infrared Absorption in Symmetric Squarylium and Croconate Dyes: A Comparative Study Using Symmetry-Adapted Cluster-Configuration Interaction Methods. *J. Phys. Chem. A* **2005**, *109*, 8604−8616.
(48) Yesudas, K.; Krishna Chaitanya, G.; Prabhakar, Ch.; Bhanuprakash, K.; Jayathirtha Rao, V. Structure, Bonding, and Lowest Energy Transitions in Unsymmetrical Squaraines: A Computational Study. *J. Phys. Chem. A* **2006**, *110*, 11717−11729.
(49) Yesudas, K.; Bhanuprakash, K. Origin of Near-Infrared Absorption and Large Second Hyperpolarizability in Oxyallyl Diradicaloids: A Three-State Model Approach. *J. Phys. Chem. A* **2007**, *111*, 1943−1952.
(50) Fabian, J. TDDFT-Calculations of Vis/NIR Absorbing Compounds. *Dyes Pigm.* **2009**, *84*, 36−53.
(51) Terenziani, F.; Painelli, A.; Katan, C.; Charlot, M.; Blanchard-Desce, M. Charge Instability in Quadrupolar Chromophores: Symmetry Breaking and Solvatochromism. *J. Am. Chem. Soc.* **2006**, *128*, 15742−15755.
(52) Sissa, C.; Terenziani, F.; Painelli, A.; Bhaskar Kanth Siram, R.; Patil, S. Spectroscopic Characterization and Modeling of Quadrupolar Charge-Transfer Dyes with Bulky Substituents. *J. Phys. Chem. B* **2012**, *116*, 4959−4966.
(53) Improta, R.; Barone, V.; Santoro, F. Ab Initio Calculations of Absorption Spectra of Large Molecules in Solution: Coumarin C153. *Angew. Chem., Int. Ed.* **2007**, *46*, 405−408. Barone, V.; Improta, R.; Rega, N. Quantum Mechanical Computations and Spectroscopy: From Small Rigid Molecules in the Gas Phase to Large Flexible Molecules in Solution. *Acc. Chem. Res.* **2008**, *41*, 605−616. Barone, V.; Bloino, J.; Biczysko, M.; Santoro, F. Fully Integrated Approach to Compute Vibrationally Resolved Optical Spectra: From Small Molecules to Macrosystems. *J. Chem. Theory Comput.* **2009**, *5*, 540−554. Lin, N.; Luo, Y.; Ruud, K.; Zhao, X.; Santoro, F.; Rizzo, A. Differences in Two-Photon and One-Photon Absorption Profiles Induced by Vibronic Coupling: The Case of Dioxaborine Heterocyclic Dye. *ChemPhysChem* **2011**, *12*, 3392−3403.
(54) Olsen, S.; McKenzie, R. H. A Diabatic Three-State Representation of Photoisomerization in the Green Fluorescent Protein Chromophore. *J. Chem. Phys.* **2009**, *130*, 184302−184314. Olsen, S. A Modified Resonance-Theoretic Framework for Structure−Property Relationships in a Halochromic Oxonol Dye. *J. Chem. Theory Comput.* **2010**, *6*, 1089−1103. Olsen, S.; McKenzie, R. H. Bond Alternation, Polarizability, and Resonance Detuning in Methine Dyes. *J. Chem. Phys.* **2011**, *134*, 114520−114532. Olsen, S. Four-Electron, Three-Orbital Model for the Low-Energy Electronic Structure of Cationic Diarylmethanes: Notes on a "Pauling Point. *J. Phys. Chem. A* **2012**, *116*, 1486−1492.
(55) Painelli, A. Vibronic Contribution to Static NLO Properties: Exact Results for the DA Dimer. *Chem. Phys. Lett.* **1998**, *285*, 352−358. Painelli, A. Amplification of NLO Responses: Vibronic and Solvent Effects in Push−Pull Polyenes. *Chem. Phys.* **1999**, *245*, 185−197.
(56) Painelli, A.; Terenziani, F. A Non-Perturbative Approach to Solvatochromic Shifts of Push−Pull Chromophores. *Chem. Phys. Lett.* **1999**, *312*, 211−220.
(57) Painelli, A.; Terenziani, F. Optical Spectra of Push−Pull Chromophores in Solution: A Simple Model. *J. Phys. Chem. A* **2000**, *104*, 11041−11048. Terenziani, F.; Painelli, A.; Comoretto, D. Solvation Effects and Inhomogeneous Broadening in Optical Spectra of Phenol Blue. *J. Phys. Chem. A* **2000**, *104*, 11049−11054.

(58) Boldrini, B.; Cavalli, E.; Painelli, A.; Terenziani, F. Polar Dyes in Solution: A Joint Experimental and Theoretical Study of Absorption and Emission Band Shapes. *J. Phys. Chem. A* **2002**, *106*, 6286−6294.
(59) Grisanti, L.; Sissa, C.; Terenziani, F.; Painelli, A.; Roberto, D.; Tessore, F.; Ugo, R.; Quici, S.; Fortunati, I.; Garbin, E.; et al. Enhancing the Efficiency of Two-Photon Absorption by Metal Coordination. *Phys. Chem. Chem. Phys.* **2009**, *11*, 9450−9457.
(60) Terenziani, F.; Sissa, C.; Painelli, A. Symmetry Breaking in Octupolar Chromophores: Solvatochromism and Electroabsorption. *J. Phys. Chem. B* **2008**, *112*, 5079−5087. Campo, J.; Painelli, A.; Terenziani, F.; Regemorter, T. V.; Beljonne, D.; Goovaerts, E.; Wenseleers, W. First Hyperpolarizability Dispersion of the Octupolar Molecule Crystal Violet: Multiple Resonances and Vibrational and Solvation Effects. *J. Am. Chem. Soc.* **2010**, *132*, 16467−16478.
(61) Sissa, C.; Painelli, A.; Blanchard-Desce, M.; Terenziani, F. Fluorescence Anisotropy Spectra Disclose the Role of Disorder in Optical Spectra of Branched Intramolecular-Charge-Transfer Molecules. *J. Phys. Chem B* **2011**, *115*, 7009−7020.
(62) Terenziani, F.; Przhonska, O. V.; Webster, S.; Padilha, L. A.; Slominsky, Y. L.; Davydenko, I. G.; Gerasov, A. O.; Kovtun, Y. P.; Shandura, M. P.; Kachkovski, A. D.; et al. A. Essential-State Model for Polymethine Dyes: Symmetry Breaking and Optical Spectra. *J. Phys. Chem. Lett.* **2010**, *1*, 1800−1804.
(63) Keil, D.; Hartmann, H. Synthesis and Characterization of a New Class of Unsymmetrical Squaraine Dyes. *Dyes Pigm.* **2001**, *49*, 161−179.
(64) Salice, P.; Arnbjerg, A.; Wett Pedersen, B.; Tofteegard, R.; Beverina, L.; Pagani, G. A.; Ogilby, P. R. Photophysics of Squaraine Dyes: Role of Charge-Transfer in Singlet Oxygen Production and Removal. *J. Phys. Chem. A* **2010**, *114*, 2518−2525.
(65) Law, K.-Y. Squaraine Chemistry: Effects of Structural Changes on the Absorption and Multiple Fluorescence Emission of Bis[4-(dimethylamino)phenyl]squaraine and Its Derivatives. *J. Phys. Chem.* **1987**, *91*, 5184−5193.
(66) Katan, C.; Charlot, M.; Mongin, O.; Le Droumaguet, C.; Jouikov, V.; Terenziani, F.; Badaeva, E.; Tretiak, S.; Blanchard-Desce, M. Simultaneous Control of Emission Localization and Two-Photon Absorption Efficiency in Dissymmetrical Chromophores. *J. Phys. Chem. B* **2010**, *114*, 3152−3169.
(67) Ponterini, G.; Vanossi, D.; Momicchioli, F. Chemical Asymmetry and α and β Polarizabilities of D-A-D′ Chromophores: a Three-State-Model and TDDFT-SOS Analysis of a Penta-Heptamethine Ketocyanine. *Phys. Chem. Chem. Phys.* **2012**, *14*, 4171−4180.
(68) Sissa, C.; Mohamadzadeh Jahani, P.; Soos, Z. G.; Painelli, A. Essential State Model for Two-Photon Absorption Spectra of Polymethine Dyes. *ChemPhysChem* **2012**, *13*, 1−7.
(69) Sissa, C.; Terenziani, F.; Painelli, A.; Abbotto, A.; Bellotto, L.; Marinzi, C.; Garbin, E.; Ferrante, C.; Bozio, R. Dimers of Quadrupolar Chromophores in Solution: Electrostatic Interactions and Optical Spectra. *J. Phys. Chem. B* **2010**, *114*, 882−893.
(70) Grisanti, L.; Terenziani, F.; Sissa, C.; Cavazzini, M.; Rizzo, F.; Orlandi, S.; Painelli, A. Polar Fluorenes and Spirobifluorenes: Fluorescence and Fluorescence Anisotropy Spectra. *J. Phys. Chem. B* **2011**, *115*, 11420−11430.
(71) Liptay, W. In *Excited States*; Lim, E. C., Ed.; Academic Press: New York, 1974; p 129.
(72) Reichardt, C. Solvatochromic Dyes as Solvent Polarity Indicators. *Chem. Rev.* **1994**, *94*, 2319−2358.